Chinese Chemical Letters 37 (2026) 111519

Contents lists available at ScienceDirect

Chinese Chemical Letters

journal homepage: www.elsevier.com/locate/cclet

Rational design of phenanthridine-based AIEgens for organelle-specific imaging: A dual-functional strategy *via* free amine modulation and carbon-insertion π-extension

Si-Fu Gao[a], Qiang-Qiang Li[a,*], Xing Li[a], Zi-Qiang Zhang[a], Huanan Huang[b,*], Jun Xuan[a,c,*]

[a] Anhui Province Key Laboratory of Chemistry for Inorganic/Organic Hybrid Functionalized Materials, College of Chemistry & Chemical Engineering, Anhui University, Hefei 230601, China
[b] College of Chemistry and Chemical Engineering, Jiangxi Province Engineering Research Center of Ecological Chemical Industry, Jiujiang Key Laboratory of Organosilicon Chemistry and Application, Xinghuo Organosilicon Industry Research Center, Jiujiang University, Jiujiang 332005, China
[c] Key Laboratory of Structure and Functional Regulation of Hybrid Materials (Anhui University), Ministry of Education, Hefei 230601, China

ARTICLE INFO

Article history:
Received 29 April 2025
Revised 25 June 2025
Accepted 26 June 2025
Available online 27 June 2025

Keywords:
Visible-light irradiation
Carbon-insertion
Phenanthridine luminogens
Aggregation-induced emission
Fluorescent imaging

ABSTRACT

Phenanthridine-based luminogens are known for their exceptional opto-electronic properties. They have been used in fluorescent materials as well as in biological fields. However, traditional methods for constructing the phenanthridine scaffold typically require pre-functionalized starting materials, photosensitizers or noble transition metals, which will complicate the synthesis and increase the cost. In this study, we introduce an efficient and metal-free approach to synthesize the phenanthridine derivates from free amines under visible-light irradiation. The phenanthridine ring is formed through a carbon insertion π-extension strategy. Significantly, rational design of the leaving group for the carbon-insertion reactions plays a crucial role. We successfully synthesized phenanthridine-based luminogens (DPA-Phen, MeO-DPA-Phen, and DMA-DPA-Phen). These luminogens display robust aggregation-induced emission (AIE) characteristics. Notably, they selectively localize within the lipid droplets (LDs) of tumor cells, demonstrating the potential of phenanthridine-based frameworks as viable LDs-selective fluorescent probes.

© 2026 Published by Elsevier B.V. on behalf of Chinese Chemical Society and Institute of Materia Medica, Chinese Academy of Medical Sciences.

Phenanthridine derivatives have widely appeared in fluorescent materials, which garnered significant attentions from the researchers [1–8]. These compounds exhibit superior opto-electronic properties, making them highly valuable in material fields. Naphthophenanthridine (Fig. 1A, **a1**), a special type of discotic liquid crystal, possesses high polarizability attributed to its disk-like shape and columnar stacking mode [9]. This compound supports nonlinear absorption across both visible and infrared regions, with its nonlinear optical properties being further enhanced when integrated with nanoparticles. (Dimethylamino)phenanthridine derivate **a2** (Fig. 1A) serves as a two-photon-sensitive photocage, where the 7,9-dimethoxyl substitutes enhance the uncaging efficiency [10], This feature enables its potential application in the controlled release of bioactive agents *via* light-mediated bond cleavage. Additionally, the phenanthridine-based thermally activated delayed fluorescence (TADF) emitter **a3** demonstrates high external quantum efficiency, holding promise for being used as blue fluorescent emitters in organic light-emitting devices (OLEDs) [11–13].

Phenanthridine derivatives also exhibit a wide range of biological activities. The phenanthridinium-based alkaloid chelerythrine (Fig. 1B, **b1**) can act as a selective antagonist of the Ca^{2+}/phospholipid-dependent protein kinase from the rat brain [14]. It selectively inhibits both the native protein kinase C (PKC) and the fragment identically without affecting [^{3}H]-phorbol-12,13-dibutyrate binding to PKC. The phenanthridinium salts also serve as the trypanocides. Among them, ethidium bromide (**b2**) are more effective than the simple phenanthridinium species due to their enhanced trypanocidal activity, lower toxicity and photosensitizing effects [15,16]. Both of the ethidium (**b2**) and trispheridine (**b3**) could act as the DNA interclator which have been widely used as the fluorescent probes to visualize DNA transactions for both *in vivo* or *in vitro*. Additionally, phenanthridine-containing luminogens like PTMM (**b4**) play a significant role in biomedical fluorescent imaging for their aggregation-induced emission characteristics [17–19]. Some donor-acceptor (D-A) type molecules with phenanthridine scaffold can be used for dynamic monitoring of viscosity

* Corresponding authors.
E-mail addresses: liqiangqiang@ahu.edu.cn (Q.-Q. Li), huanan200890@163.com (H. Huang), xuanjun@ahu.edu.cn (J. Xuan).

https://doi.org/10.1016/j.cclet.2025.111519
1001-8417/© 2026 Published by Elsevier B.V. on behalf of Chinese Chemical Society and Institute of Materia Medica, Chinese Academy of Medical Sciences.

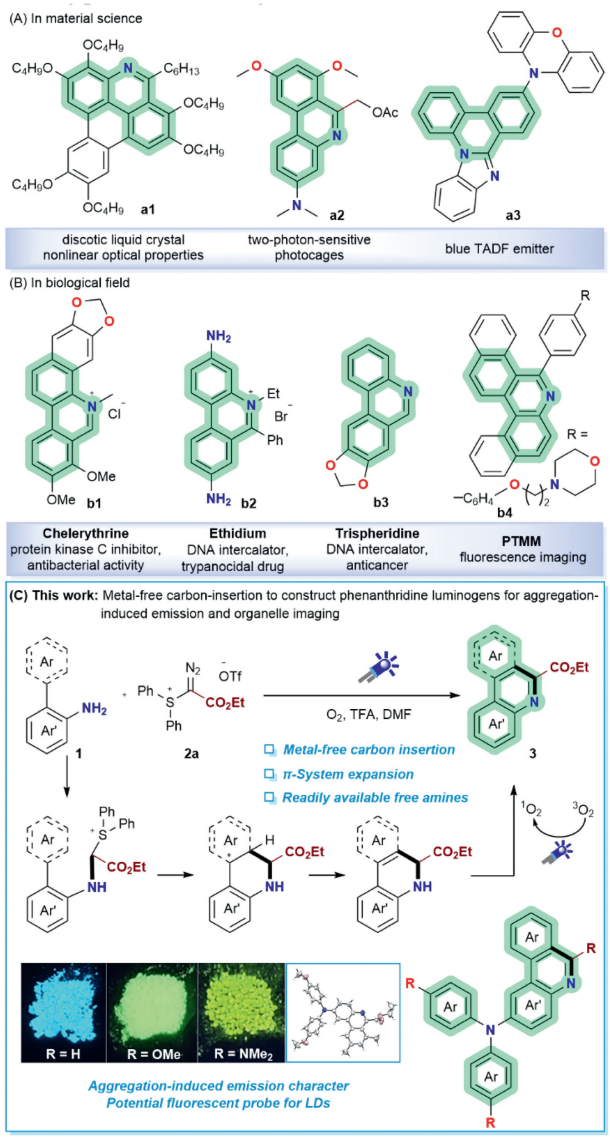


Fig. 1. (A) Utilization of phenanthridine derivatives in the field of material science. (B) Utilization of phenanthridine derivatives in biological field. (C) Our synthetic design.

fluctuations during mitophagy, owing to their good biocompatibility and low cytotoxicity [20].

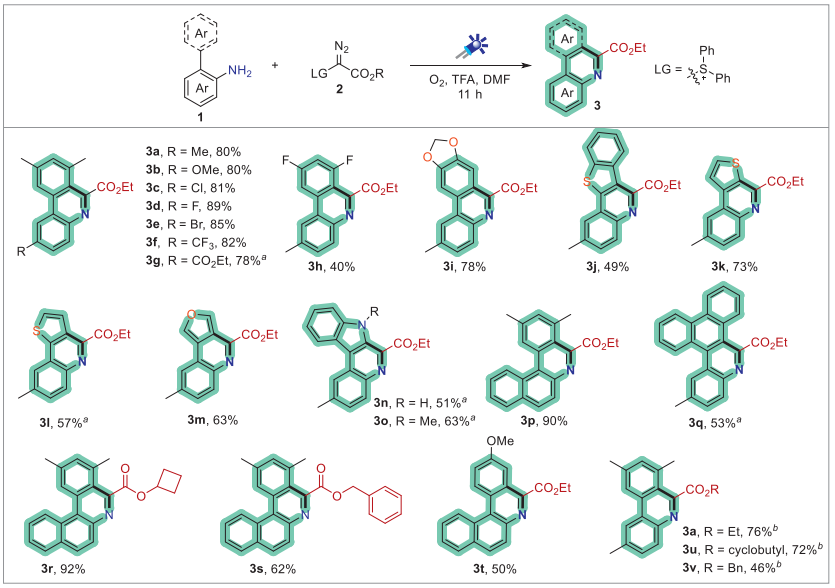
To obtain the phenanthridine-containing molecules, the key point is to construct the specific phenanthridine rings [21,22]. A widely adopted method for constructing the phenanthridine scaffold is the cascade radical addition-cyclization of 2-isocyano-1,1′-biphenyl [23–31]. However, the starting material isocyanides often require multi-step syntheses and emit a strong, unpleasant odor, making them inconvenient to be handled. Another approach for phenanthridine scaffold involves metal-catalyzed annulation of various functional. molecules such as imidoyl chlorides [25,32–34], oximes [16,35–37], imines [3,38–41]. This process typically employs metal-catalyzed C–H arylation for intramolecular reactions or tandem Suzuki/C–H arylation for intermolecular reaction. Phenanthridine derivates can also be synthesized from amides *via* Morgan-Wall reactions, which generally necessitate the use of strong Lewis acids [42–44]. Additionally, there are several examples of using olefins as the one-carbon synthon for the cross-ring-annulation reaction based on C–H bond activation. However, these reactions involve C=C bond cleavage, which is notoriously challenging and typically requires transition metals and high temperatures [45–47]. It should be noticed that the annulation reaction of 2-arylanilines to synthesize phenanthridines had ever been reported [47]. In these studies, benzoyl groups were used as one of the leaving groups, and C–C bond cleavage was required, both of which led to the high temperature conditions.

Despite these progresses in constructing the phenanthridine scaffold, the existing methods often require pre-functionalized starting materials, and usually necessitate the use of radical initiators or noble transition metals. These would lead to facing complex raw material preparation issues, high cost of the noble metals and the corresponding metal recycling problems.

Based on the current research state, it is imperative to develop a new method by using easily obtainable starting materials and moderate conditions to construct the phenanthridine structure. In order to achieve this goal, carbon-insertion ring expansion strategy is used. The readily available free amines without any protecting groups are preferred instead of the pre-functionalized ones. However, the big challenge is how to realize the carbon insertion with more moderate conditions. A suitable reagent as the one-carbon synthon has become the key point to solve the problem. Considering the characteristics of the reaction, leaving groups with suitable activity of the carbon-insertion reagent is essential. Diazo compounds are of significant importance in organic synthesis owing to their utility as versatile synthetic intermediates [48–51]. Based on our ongoing research interests in light-promoted transformation of diazo molecules and the carbon-insertion ring expansion strategy, in this research, we reported herein the synthesis of phenanthridine luminogens by using bifunctional α-diazo sulfonium compounds and biaryl-2-amines (Fig. 1C). α-Diazo sulfonium compounds have proved to be effective as the carbon synthon by using diazo and thioether as the suitable leaving groups [52–60].

Trimethyl-[1,1′-biphenyl]−2-amine (**1a**) and α-diazo sulfonium salt (**2a**) were utilized as the starting materials to explore the carbon-insertion π-extension reaction. Both of light and acid were identified as essential components for the reaction (Table S1 in Supporting information, entries 2 and 3). The reaction was compatible with various solvents, yet *N*,*N*-dimethylformamide (DMF) exhibited higher reactivity (Table S1, entry 4 to entry 9). The molar ratio of the starting materials was also investigated, revealing that excess of **2a** enhanced the reaction yield (Table S1, entries 10 and 11). This improvement might be attributed to the instability of α-diazo sulfonium salt under acidic conditions. Consequently, the optimized reaction conditions were then established as follows: **1a** (0.30 mmol), **2a** (0.90 mmol), trifluoroacetic acid (TFA)/DMF (4:1), irradiation by 24 W blue LEDs (λ_{max} = 455 nm) at room temperature for 11 h under an oxygen atmosphere (Table S1, entry 1).

With the standard reaction conditions established, the scope of amines was initially explored. The substrates (**1**) bearing various *para*-substituents of amino afforded moderate to good yields (Scheme 1), encompassing both electron-donating groups (EDG) (**3a**, **3b**) and electron-withdrawing groups (**3f**, **3g**). The halogenated amines were particularly active, yielding the halogenated phenanthridines in good yields (**3c**–**3e**), which were valuable synthetic synthons for molecular modification *via* coupling reactions. It would be convenient to synthesize the substituted trisphaeridine (**3i**) by this method, which was a naturally occurring alkaloid with applications in the pharmaceutical research for alkaloid studies [61,62]. However, when the two methyl groups were replaced by fluorine atoms (**3h**), the reaction yield decreased, likely due to the electron-withdrawing nature of fluorine. On the contrary, the electron-rich heteroaromatic rings like benzothiophenyl (**3j**), thienyl (**3k**, **3l**), furyl (**3m**), indolyl (**3n**, **3o**) provided moderate to good yields. Additionally, substrates containing polycyclic aromatics substitutes, conjugated π-expansion molecules could be obtained under the standard conditions (**3p**, **3q**), which are known



Scheme 1. Substrate scope of amines. Reaction conditions: **1** (0.30 mmol), **2a** (0.90 mmol), TFA/DMF (4:1), irradiation by 24 W blue LEDs (455 nm) at room temperature for 11 h under oxygen atmosphere, isolated yield. [a] LG = -I(OTf)Ph. [b] Determined by ^{1}H NMR.

for their unique optical and electronic properties. The scope of diazo reagents was also investigated (Scheme 1). Various esters, including cyclobutyl, benzyl and ethyl, were found to be active (**3r**, **3s**, **3t**). Furthermore, diazo iodine(III) compounds were also tested and provided moderate to good yields (**3u**, **3v**, **3a**). However, due to the preparation difficulty of α-diazo sulfonium, primarily attributed to its purification and low isolation yields, the substrate scope of this class of compounds has been primarily restricted to those bearing ester functional groups, such as ethyl, cyclobutyl or benzyl ester derivatives. Additionally, the majority of reaction yields obtained remain moderate, typically ranging from 40 % to 92 %, which has posed challenges for their broader synthetic transformation.

The phenanthridine-containing polycyclic aromatic hydrocarbons (PAHs) typically display distinct opto-electronic characteristics [21,22]. To investigate the optical properties of the phenanthridines (Phen), their emission spectra were measured (Fig. 2A). Due to the resemblance in molecular frameworks and the presence of weak intermolecular interactions (such as π-π stacking) in solution, the fluorescence spectra of most compounds were similar. Compound **3o** exhibited the biggest emission peak among them. This phenomenon may be attributed to the strong electron-donating ability of pyrrole and the extended π-conjugated system, which could lower the molecular energy gap and result in a significant redshift. In contrast to the emission in solution, the emission spectra in solid state exhibited stronger intermolecular interaction and more produced differences among the compounds. As illustrated in Fig. 2B (solid-state fluorescence spectra), ethyl 2,7,9-trimethylphenanthridine-6-carboxylate (**3a**) displayed an emission spectrum ranging from 360 nm to 550 nm, with the highest peak at 391 nm. 2-Electron-withdrawing group (EWG)-substituted phenanthridines (**3c**, **3f**) showed similar signals compared with **3a**. However, red-shift fluorescence emission was observed for electron-rich (hetero)arene-fused phenanthridines (**3i**, **3k**, **3l**, **3o**, **3p**, **3q**). This observation suggested that EDG and the EWG picolinate of the phenanthridine derivates formed the push–pull chromophores. The EDG increased the electron density associated with the aromatic ring to the conjugated system, while the EWG decreased it, facilitating efficient intramolecular charge transfer (ICT) from the donor to the acceptor. The ICT process lowers the energy of the excited state, leading to a redshift in the emission spectra [63]. It is intriguing to note that the fluorescence spectra of **3l** and **3k** were different, likely due to the different conjugation effects caused by the varying positions of thiophene group.

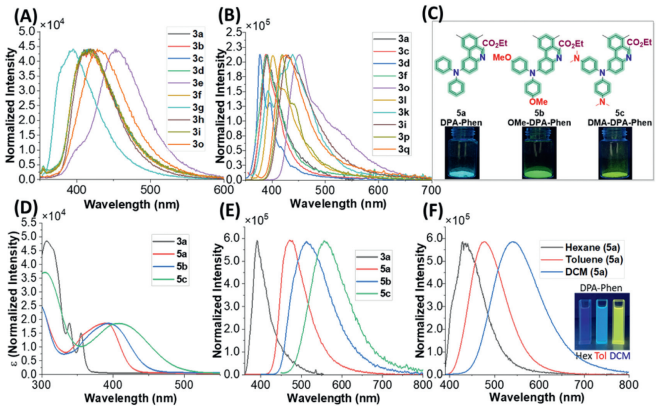
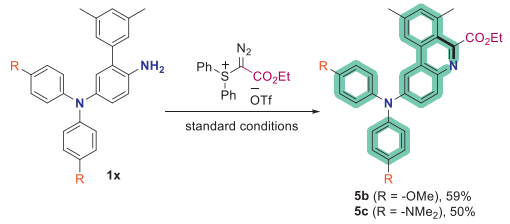


Fig. 2. (A) Fluorescence spectra of the phenanthridines in dichloromethane, excitation wavelength: 330 nm for **3o** and 320 nm for other compounds, concentration: 1.0×10^{-5} mol/L. (B) Solid fluorescence spectra of the phenanthridines, excitation wavelength: 320 nm for **3i**, **3o** and **3p**; 330 nm for **3a**; 345 nm for **3c**, **3d** and **3l**; 350 nm for **3f** and **3k**; 360 nm for **3q**. (C) The fluorescence photographs of **5a**, **5b** and **5c** in sold state. (D) UV–vis spectra of **3a** (1.8×10^{-4} mol/L), **5a**, **5b**, **5c** (1.8×10^{-5} mol/L). (E) Solid fluorescence spectra of **3a**, **5a**, **5b**, **5c**, excitation wavelength: 330 nm for **3a** and **5a**, 390 nm for **5b**, 410 nm for **5c**. (F) Normalized solvent-dependent fluorescence spectra of **5a** in *n*-hexane (black), toluene (red), dichloromethane (blue) solutions at 1.0×10^{-5} mol/L, excitation wavelength: 380 nm (inset: fluorescent photographs of DPA-Phen in different solvents).

The variations in emission spectra resulting from electron-donating and electron-withdrawing groups spurred our initiative to design novel push-pull chromophores and explore their practical applications. Given the electron-deficient nature of the phenanthridine structure and the pre-existing electron-withdrawing ester groups, we endeavored to introduce several representative EDG to the phenanthridine skeleton to construct new chromophores with robust push-pull capabilities. The diarylamine, serving as a new donor unit was incorporated into the starting materials (Fig. 2C). Under the standard conditions, the products MeO-DPA-Phen (**5b**) and DMA-DPA-Phen (**5c**) were successfully synthesized in a direct manner from the corresponding free amines, achieving yields of



Scheme 2. Design and synthesis of phenanthridine-based AIEgens.

59 % and 50 %, respectively (Scheme 2). DPA-Phen (**5a**) could be obtained in 62 % yield through a coulping reaction from bromo–substituted phenanthridine and diphenylamine, while the yield would be much lower when using the free amine method [64]. As anticipated, all of them exhibited distinct photoluminescent properties in solid state with the irritation of 365 nm fluorescence lamp irradiation (Fig. 2C, blue for **5a**, green for **5b**, yellow for **5c**), and the quantum yields (QY) of **5a**, **5b** and **5c** in solid state were 93.8 %, 47.2 %, and 2.9 % respectively. Their photostability was also evaluated, and the results indicated that they exhibited good photostability (Fig. S3 in Supporting information).

To further investigate their optical properties, the absorption (Fig. 2D) and solid fluorescence spectra (Fig. 2E) were tested. As shown in Figs. 2D and E, a stronger donor ability led to a larger red shift. DMA-DPA-Phen (**5c**) exhibited broadabsorption at $\lambda = 300$–550 nm with discrete major peaks at 305 and 409 nm, and emission at $\lambda = 450$–800 nm with a major peak at 559 nm, which are higher than those of DPA-Phen (**5a**) and MeO-DPA-Phen (**5b**). Additionally, thesolvatochromic effect of DPA-Phen (**5a**) was studied. The fluorescence spectra showed a significant redshift with increasing the solvent polarity. This can be attributed to the ICT character for the push–pull chromophore [65,66]. The ICT effect would make the excited state more polar than the ground state, with a formal positive charge on the donor and a negative charge on the acceptor. Thus, the polar solvents can better stabilize the excited state, leading to positive solvatochromism [67]. DPA-Phen (**5a**) exhibited different fluorescence colors in various solvents (the inset of Fig. 2F). Their electronic distribution of highest occupied molecular orbital (HOMO) and lowest unoccupied molecular orbital (LUMO) were studied theoretically by density functional theory (DFT) calculations at the level of B3LYP/6–31g(d)* (Fig. S6 in Supporting information). The results demonstrate that as the donor ability of the substituents strengthens, the HOMO-LUMO energy gap widens, causing a red shift in emission from **5a** to **5c**. Moreover, the calculation also reveals ICT can take place between the strong electron-donating benzene ring and the phenanthridine moiety.

To further study the optical properties of the new push–pull chromophores (**5a**, **5b** and **5c**), additional experiments were conducted. The fluorescence spectra of DMSO solutions were initially measured. Upon photoexcitation, a weak fluorescence signal was observed for DPA-Phen (**5a**), while negligible signals were detected for MeO-DPA-Phen (**5b**) and DMA-DPA-Phen (**5c**). The QY of compounds **5a**, **5b**, **5c** in solution are 90.6 % (in DCM), 49.6 % (in toluene), 13.8 % (in hexane), respectively. Subsequently, water, as a poor solvent was added in batches into the DMSO solution. As depicted in Figs. 3A–C, adding water with a volume fraction of below 50 % to the DMSO solutions did not significant alter the emission spectra. However, dramatic enhancement in fluorescence intensity was observed when the water fraction reached 50 %–60 %, and the intensity remained in a high level with further addition of water. These observations were the characteristic of the aggregation-induced emission (AIE) effect [68–72]. The viscosity-dependent fluorescence test of **5c** was also performed (Fig. S5 in Supporting information). We restricted their rotations by increasing the glycerol to methanol volume ratio. It was observed that the photoluminescence intensity increased with the increase of the glycerol/ethanol ratio. This finding is in consistent with the prediction of the aggregation-induced emission (AIE) effect. To confirm this phenomenon, the luminescent changes were monitored during the evaporation of a drop of the dichloromethane solution of **5a**, **5b** and **5c** on a thin-layer chromatography plate (Fig. 3D). As the solvent evaporated, **5a** exhibited bright yellow luminescence, which gradually shifted to blue. For **5b** and **5c**, the luminescence intensity progressively increased with aggregation on the thin-layer chromatography plate under 365 nm fluorescence lamp irradiation. These results indicated that **5b** and **5c** exhibit a typical AIE effect.

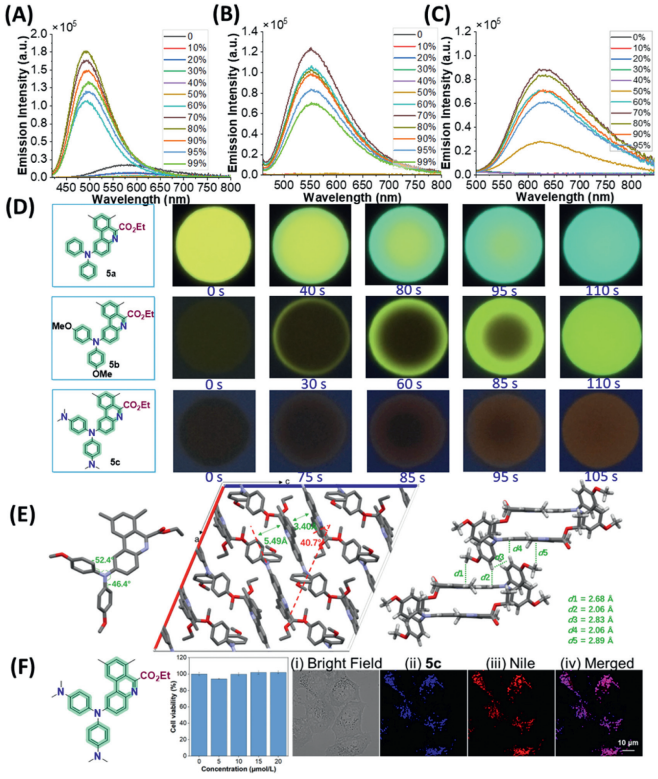


Fig. 3. (A) Photoluminescence spectra of **5a** (1.0×10^{-5} mol/L) in DMSO/H_2O mixtures with different water fractions, excitation wavelength: 410 nm. (B) Photoluminescence spectra of **5b** (1.0×10^{-5} mol/L) in DMSO/H_2O mixtures with different water fractions, excitation wavelength: 450 nm. (C) Photoluminescence spectra of **5c** (1.0×10^{-5} mol/L) in DMSO/H_2O mixtures with different water fractions, excitation wavelength: 450 nm. (D) Photos of one drop of **5a**, **5b**, **5c** solution in DCM on the thin layer chromatography plate with different evaporation timescales at room temperature (under irradiation with 365 nm UV lamp). (E) The crystal packing structure of **5b**. (F) Cell toxicity effect of **5c** to HeLa cell and confocal fluorescence images of HeLa cells stained with CellMask Nile red (5 μmol/L) and **5c** (10 μmol/L). Images of (i) bright field image, (ii) **5c** (excitated with 405 nm laser) and (iii) Nile red (excitated with 543 nm laser). (iv) Merged bright field images of Nile red and **5c** (Pearson's correlation coefficient: 0.902). Data are presented as mean ± standard deviation (SD) ($n = 3$).

To elucidate the cause of the typical AIE behavior exhibited by the compounds, we attempted to obtain their single crystals for structure analysis. Single crystals of **5a** (CCDC: 2428585) and **5b** (CCDC: 2428588) suitable for X-ray crystallography analysis were successfully obtained by slow diffusion of petroleum ether into a dichloromethane solution under argon at room temperature, while **5c** resisted all attempts at crystallization. The X-ray diffraction analysis elucidated that **5b** crystallized in monoclinic space group *C*2/*c*, with eight molecules in one cell unit. For a single molecule, the torsion angles between the parent phenanthridine core and the two phenyl rings at thenitrogen position were −52.4° and −46.4°

(Fig. 3E). Within the unit cell, two intermolecular phenanthridine rings faced with each other. The main π core of them adopted a planar structure with a stacking distance of 3.40 Å. Additionally, the intermolecular interactions caused a "slipped" structure with an angle of 40.7° and a separation distance of 5.49 Å, which efficiently hindered the π–π stacking, thereby preventing the emission quenching. This structural feature likely contributed significantly to the enhanced AIE behavior. Moreover, the interactions between the adjacent molecules, such as C–H (OCH_3)···π, C–H (CH of phenyl)···π, with distances ranging from 2.06 Å to 2.89 Å, further restricted the molecular motion and rigidified the molecular conformation in the solid state. These factors collectively suppressed the molecular rotation and significantly strengthened the AIE effect.

The prominent AIE effect exhibited by the new push-pull chromophores motivated us to explore their practical applications. The fluorescence behavior in aqueous solution (DMSO/H_2O) suggested their potential utility in fluorescent imaging of organelles, given the similar aqueous cellular environment. Initially, the biocompatibility of **5c** was assessed with toxicology assay kit. When HeLa cells were incubated with **5c**, the treatment did not cause any drastic impact on the viabilities of the various treated cell lines, indicating relatively low toxicity of **5c** (Fig. 3F). Considering the large lipophilic substitution on the molecular skeleton of **5c**, we hypothesized that it would preferentially accumulate in the lipophilic organelles of cells upon cellular uptake. To test this hypothesis, HeLa cells incubated with **5c** were co-stained with Nile red. As shown in Fig. 3F, the merged confocal images of Nile red and **5c** showed significant colocalization within HeLa cell, confirming that **5c** mainly accumulated in the lipid droplets. This localization should be ascribed to the inherent lipophilic nature of lipid droplets. Lipid droplets serve as the storage organelles for lipids and are essential for lipid metabolism and energy homeostasis. They can also participate in the innate immune response in macrophages by storing and releasing fatty acids. Thus, their proper function is closely linked to the metabolic diseases. The development of sensitive and effective cellular probes for visualizing the lipid droplets in biological systems is highly desirable. The lipophilicity nature of **5c** and its high selectively accumulated in lipid droplets make it a promising candidate for a fluorescent cellular probe.

We have designed and synthesized the phenanthridine derivates *via* metal-free carbon-insertion π-extension strategies starting from free amines. α-Diazo sulfonium salts were chosen as the efficient carbon-insertion reagent due to their suitable leaving ability of the diazo and sulfonium groups. The resulting phenanthridine-based luminogens exhibit strong aggregation-induced emission characteristic and have been successfully applied in fluorescent organelle imaging. This approach is expected to serve as a complementary strategy for constructing phenanthridine-based frameworks. Moreover, the reduced toxicity and inherent photosensitizing properties of phenanthridine derivatives are poised to render this method highly appealing in both fluorescent materials research and biological applications, thereby fostering its widespread adoption across these disciplines.

Declaration of competing interest

The authors declare that they have no known competing financial interests or personal relationships that could have appeared to influence the work reported in this paper.

CRediT authorship contribution statement

Si-Fu Gao: Writing – original draft, Methodology, Data curation. **Qiang-Qiang Li:** Writing – original draft, Project administration, Conceptualization. **Xing Li:** Software, Data curation. **Zi-Qiang Zhang:** Validation, Formal analysis. **Huanan Huang:** Writing – review & editing, Investigation, Conceptualization. **Jun Xuan:** Writing – review & editing, Supervision, Project administration, Conceptualization.

Acknowledgments

We are grateful to the National Natural Science Foundation of China (Nos. 21971001, 22301292 and 22261028), the Distinguished Young Research Project of Anhui Higher Education Institution (No. 2023AH020003), and the Natural Science Foundation of Anhui Province (No. 2408085MB041) for financial support of this work.

Supplementary materials

Supplementary material associated with this article can be found, in the online version, at doi:10.1016/j.cclet.2025.111519.

References

[1] B.D. Krane, M.O. Fagbule, M. Shamma, B. Gozler, J. Nat. Prod. 47 (1984) 1–43.
[2] A.A. Ali, H.M. El Saved, O.M. Abdalliah, W. Steglich, Phytochemistry 25 (1986) 2399–2401.
[3] P. Lasák, K. Motyka, V. Krystof, J. Styskala, Molecules 23 (2018) 2155.
[4] V. Bisai, M.K. Saina Shaheeda, A. Gupta, A. Bisai, Asian J. Org. Chem. 8 (2019) 946–969.
[5] X. Zhang, M.R. Mackinnon, G.J. Bodwell, S. Ito, Angew. Chem. Int. Ed. 61 (2022) e202116585.
[6] W. Wang, F. Hanindita, Y. Hamamoto, Y. Li, S. Ito, Nat. Comm. 13 (2022) 1498.
[7] W. Wang, F. Hanindita, Y. Tanaka, K, et al., Angew. Chem. Int. Ed. 62 (2023) e202218176.
[8] Y. Hamamoto, K. Ochiai, Y. Li, E. Tapavicza, S. Ito, Angew. Chem. Int. Ed. 63 (2024) e202319022.
[9] M. Joseph, S. Tomson, M. Vadivel, et al., J. Mol. Liq. 416 (2024) 126503.
[10] C.M. Attiach, A. Kumar, J. Daniel, et al., Chem. Commun. 60 (2024) 8260.
[11] T. Ohsawa, H. Sasabe, T. Watanabe, et al., Adv. Optical Mater. 7 (2019) 1801282.
[12] S. Karthik, J. Ajantha, S. Easwaramoorthi, T. Gandhi, New J. Chem. 44 (2020) 9530.
[13] J. Zhang, J.R. Lakowicz, J. Phys. Chem. B 109 (2005) 8701.
[14] J.M. Herbert, J.M. Augereau, J. Gleye, J.P. Maffrand, Biochem. Biophys. Res. Commun. 172 (1990) 993.
[15] M. Wainwright, Biotech. Histochem. 85 (2010) 341.
[16] K. Nakamura, E. Kobayashi, K. Moriyama, H. Togo, Tetrahedron 91 (2021) 132244.
[17] N. Stevens, N. O'Connor, H. Vishwasrao, et al., J. Am. Chem. Soc. 130 (2008) 7182.
[18] D. Wu, B. Fang, M. Zhang, et al., Dyes Pigm. 159 (2018) 142–150.
[19] Y. Zhang, M. Fan, Z. Xu, et al., J. Nanobiotechnol. 21 (2023) 107.
[20] H.X. Wang, J.Y. Zhao, Wang H, et al., Dyes Pigm. 232 (2025) 112479.
[21] X. Zhang, D. Li, C.C.H. Tan, et al., Nat. Synth. 3 (2024) 1283–1291.
[22] Y. Hamamoto, W. Wang, Y. Li, S. Ito, Angew. Chem. Int. Ed. 64 (2025) e202416654.
[23] B. Zhang, A. Studer, Chem. Soc. Rev. 44 (2015) 3505–3521.
[24] J. Lei, J. Huang, Q. Zhu, Org. Biomol. Chem. 14 (2016) 2593–2602.
[25] A.D. Tito, H.O. Abdulla, D. Ravelli, et al., Beilstein J. Org. Chem. 16 (2020) 1476–1488.
[26] F. Doraghi, P. Baghershahi, F. Gilaninezhad, et al., Adv. Synth. Catal. 367 (2025) e202400994.
[27] F. Doraghi, A. Amini, M. Ghanbarlou, et al., Mol. Divers. 28 (2024) 419–435.
[28] Y.J. Zhuang, J.P. Qu, Y.B. Kang, J. Org. Chem. 85 (2020) 4386–4397.
[29] X.K. He, J. Lu, H.B. Ye, L. Li, Molecules 26 (2021) 6843.
[30] H.B. Ye, X.Y. Zhou, L. Li, J. Xuan, Org. Lett. 24 (2022) 6018–6023.
[31] Y.Z. Chen, Y.M. Chen, Y. Hu, et al., Org. Lett. 25 (2023) 7518–7522.
[32] W. Fu, M. Zhu, F. Xu, et al., RSC Adv. 4 (2014) 17226.
[33] W.Y. Wang, X. Feng, B.L. Hu, et al., J. Org. Chem. 78 (2013) 6025.
[34] Z. Wang, T. Li, J. Zhao, et al., Org. Lett. 20 (2018) 6640.
[35] R.T. McBurney, A.M.Z. Slawin, L.A. Smart, et al., Chem. Commun. 47 (2011) 7974–7976.
[36] I. Deb, N. Yoshikai, Org. Lett. 15 (2013) 4254–4257.
[37] G. Raju, V. Guguloth, B. Satyanarayana, RSC Adv. 6 (2016) 45036–45040.
[38] M. Gioanola, R. Leardini, D. Nanni, et al., Tetrahedron 51 (1995) 2039.
[39] D. Shabashov, O. Daugulis, J. Org. Chem. 72 (2007) 7720–7725.
[40] J. Peng, T. Chen, C. Chen, B. Li, J. Org. Chem. 76 (2011) 9507–9513.
[41] J. Fan, L. Li, J. Zhang, M. Xie, Chem. Commun. 56 (2020) 2775.
[42] A. Pictet, A. Hubert, Ber. Dtsch. Chem. Ges. 29 (1896) 1182–1189.
[43] C.T. Morgan, L.P. Walls, J. Chem. Soc. (1931) 2447–2456.
[44] C.T. Morgan, L.P. Walls, J. Chem. Soc. (1932) 2225–2231.
[45] D. Chowdhury, S. Dana, A. Mandal, M. Baidya, Chem. Commun. 55 (2019) 11908.

[46] Y.Y. Liu, R.J. Song, C.Y. Wu, et al., Adv. Synth. Catal. 354 (2012) 347–353.
[47] P. Chen, J. Nan, Y. Hu, et al., Chem. Sci. 12 (2021) 803.
[48] W. Yang, Z. Yang, L. Chen, et al., Chin. Chem. Lett. 34 (2023) 107791.
[49] B.G. Cai, G.Y. Xu, J. Xuan, Chin. Chem. Lett. 34 (2023) 108335.
[50] H. Huang, J. Chen, L. Zhang, et al., Chin. Chem. Lett. 36 (2025) 109992.
[51] Q. Feng, J. Hao, Y. Hu, et al., Chin. Chem. Lett. 36 (2025) 110582.
[52] X. Wang, W.Y. Tong, B. Huang, et al., J. Am. Chem. Soc. 144 (2022) 4952–4965.
[53] H. Huang, X. Zou, S. Cao, et al., Org. Lett. 23 (2021) 4185–4190.
[54] X. Ren, Q. Ke, Y. Zhou, et al., Angew. Chem. Int. Ed. 62 (2023) e202302199.
[55] M.T. Taylor, J.E. Nelson, M.G. Suero, M.J. Gaunt, Nature 562 (2018) 563–568.
[56] X. Li, C. Golz, M. Alcarazo, Angew. Chem. Int. Ed. 60 (2021) 6943–6948.
[57] M.Y. He, X. Tang, H.Y. Wu, et al., Org. Lett. 25 (2023) 9041–9046.
[58] W.W. Zhao, M.Y. Tian, Y.L. Zhou, et al., Angew. Chem. Chem. Int. Ed. 63 (2024) e202318887.
[59] X.C. Xu, Y. Sang, M. Yang, et al., Org. Chem. Front. 11 (2024) 5502–5510.
[60] M. Huang, G. Wang, H. Li, et al., Green Chem. 27 (2025) 413.
[61] F. Rafiee, Appl. Organometal Chem. 31 (2017) e3820.
[62] Z. Jin, Nat. Prod. Rep. 30 (2013) 849–868.
[63] F. Quist, C.M.L. Vande Velde, D. Didier, et al., Dyes Pigm. 81 (2009) 203–210.
[64] C. Wu, P.I. Djurovich, M.E. Thompson, Adv. Funct. Mater. 19 (2009) 3157–3164.
[65] Z. Zhang, R.M. Edkins, J. Nitsch, et al., Chem. Eur. J. 21 (2015) 177–190.
[66] N. Ando, T. Kushida, S. Yamaguchi, Chem. Commun. 54 (2018) 5213–5216.
[67] C. Reichardt, Chem. Rev. 94 (1994) 2319–2358.
[68] H. Huang, L. Liu, J. Wang, et al., Chem. Sci. 13 (2022) 3129–3139.
[69] J. Wang, X. Gu, P. Zhang, et al., J. Am. Chem. Soc. 139 (2017) 16974–16979.
[70] D. Yuan, Q. Wu, D. Wang, B.Z. Tang, Angew. Chem. Int. Ed. 60 (2021) 15724–15742.
[71] J. Dai, W. Wei, C. Yan, et al., Nat. Biomed. Eng. 9 (2025) 1632–1644.
[72] C. Yan, W. Zhu, R. Li, et al., Angew. Chem. Int. Ed. 64 (2025) e202422996.